LETTER TO THE EDITOR

Available online at www.sciencedirect.com

SCIENCE DIRECT®

Journal of Non-Crystalline Solids 337 (2004) 182–186

JOURNAL OF NON-CRYSTALLINE SOLIDS

www.elsevier.com/locate/jnoncrysol

Letter to the Editor

The nature of fluorine in amorphous silica

Randall E. Youngman *, Sabyasachi Sen

Corning Incorporated, Science and Technology Division, SP-AR-02-4, Corning, NY 14831, USA

Received 4 February 2004; received in revised form 22 March 2004
Available online 14 May 2004

Abstract

We have used solid-state nuclear magnetic resonance spectroscopy and molecular dynamics simulations to characterize the short-range structure of fluorine-doped silica glass. The fluorine atoms in a glass containing 3 wt% fluorine are found in two different structural environments. The most abundant of these is a fluorine atom bonded to a tetrahedral silicon atom, where the fluorine has replaced one of the bridging oxygens and formed the usual Q^3 species. The second, and less abundant of these fluorine types, originates from fluorine bonded to a silicon atom with four bridging oxygen atoms, ultimately giving rise to a fivefold coordinated silicon atom. Additional insight into these Si–F bonding configurations was obtained in the simulation results.

PACS: 61.18.Fs; 61.43.Bn; 61.43.Fs; 82.56.Ub

1. Introduction

Amorphous silica (a-SiO_2) can be doped with small quantities of fluorine, giving the resulting glass several unique and useful attributes. Since fluorine is one of only two additives (the other being boron) that lowers the refractive index of silica, it is commonly used in controlling index profiles in optical fiber [1,2]. Fluorine also lowers the dielectric constant of silica, making F-doped silica the preferred dielectric in microprocessors and logic devices [3]. This versatile material is also being considered as a photomask substrate for deep ultraviolet (157 nm) photolithography applications [4,5] and has been investigated for use in catalysis [6]. The physico-chemical and structural role of fluorine and its solubility in natural magmas is an important research area in geochemistry [7–10].

There are limited reports on the atomic structure of F-doped a-SiO_2, mostly involving vibrational spectroscopy. Raman spectroscopic studies have shown that addition of fluorine to a-SiO_2 results in a new band near 945 cm^{-1}, assigned to an Si–F stretching mode [11,12]. To our knowledge, there is only one published report on a detailed study of F-doped a-SiO_2 using nuclear magnetic resonance (NMR) spectroscopy. Duncan and co-workers utilized wideline ^{19}F NMR to identify the $SiO_{3/2}F$ configuration in the glass, due to replacement of one bridging oxygen atom with a non-bridging fluorine [13].

We report here a detailed structural analysis of F-doped silica glass which reveals for the first time the presence of multiple fluorine environments. Si–F bonding in this material occurs through the formation of $SiO_{3/2}F$ and $SiO_{4/2}F$ polyhedra, where the silicon atoms are surrounded by three or four bridging oxygens, respectively, and a single non-bridging fluorine. The latter structural unit (i.e. $SiO_{4/2}F$) is the first evidence for fivefold coordinated silicon atoms in doped vitreous silica and may have far-reaching implications in understanding a wide range of physico-chemical properties of this important material.

2. Experimental

The F-doped silica glass was obtained from Heraeus (Fluosil®) and used without further modification. The fluorine content of 3 wt% was determined by electron probe micro-analysis. The glass sample was finely powdered and packed into appropriately sized zirconia rotors for NMR spectroscopic analysis.

^{19}F wideline and magic-angle spinning (MAS) NMR data were collected using a commercial spectrometer

* Corresponding author. Tel.: +1-607 974 2970; fax: +1-607 974 9474.
E-mail address: youngmanre@corning.com (R.E. Youngman).

0022-3093/$ - see front matter © 2004 Elsevier B.V. All rights reserved.
doi:10.1016/j.jnoncrysol.2004.03.122

(Chemagnetics) in conjunction with a 4.7 T superconducting magnet (Oxford; 188.0 MHz resonance frequency for ^{19}F). These experiments were performed with a 4 mm triple-resonance MAS NMR probe and a sample spinning rate of nominally 17 kHz. The ^{19}F wideline NMR spectrum was obtained using the same MAS NMR probe, but without sample spinning. Due to the extremely long spin-lattice relaxation times (T_1) for ^{19}F in this glass, the ^{19}F NMR data were acquired using relatively short radio-frequency pulse widths of 3 μs, corresponding to a tip angle of $\pi/4$, and recycle delays of 1800–3000 s. These data were processed with minimal line broadening (~100 Hz) and plotted against the chemical shift of $CFCl_3$.

^{29}Si MAS NMR data were also collected at 4.7 T (39.7 MHz resonance frequency), using a 9.5 mm double-resonance MAS NMR probe and a sample spinning rate of 4 kHz. The ^{19}F-decoupled ^{29}Si MAS NMR spectrum was obtained using $\pi/4$ pulse widths of 3 μs and recycle delays of 900 s. The $^{19}F \rightarrow {}^{29}Si$ cross-polarization MAS (CPMAS) NMR experiments were performed using the standard Hartmann–Hahn matching approach. Parameters for these experiments included a $\pi/4$ pulse width of 3 μs for ^{19}F, recycle delays of 180 s and several different values for the contact time between the two nuclides. All ^{29}Si NMR spectra were processed with 50 Hz exponential line broadening and plotted against the chemical shift of tetramethylsilane (TMS).

The MD simulations were performed on a system of 652 atoms with 216 Si, 428 O and 8 F atoms in the simulation cell, equivalent to a composition of ~1.2 wt% fluorine in silica. Initial coordinates of the atoms were chosen randomly inside a cubic cell with lengths of ~21.4 Å. A micro-canonical (NVE) ensemble was used. The atoms were treated as non-polarizable point charges with formal charges of −1e, +4e and −2e for F, Si and O, respectively. The empirical two-body Born–Mayer–Huggins type and three-body Stillinger–Weber type interaction potentials developed for silica and silicates by Garofilini and co-workers were used to calculate Si–O, Si–F, O–F, Si–O–Si and O–Si–O interactions [14]. The long-range electrostatic interactions between atoms were evaluated using the Ewald summation method with cubic periodic boundary conditions. The system was equilibrated at 8000 K for 50 ps followed by quenching and annealing at 6000 and 4000 K for 60 ps each and at 2000 and 300 K for 240 ps each. An integration time step of 1 fs was used for the equations of motion throughout the simulation.

3. Results and discussion

The ^{19}F MAS NMR spectrum in Fig. 1(a) shows for the first time, the presence of multiple fluorine environments in F-doped a-SiO_2. If one assumes Gaussian line shapes, this spectrum can be simulated with two overlapping resonances with chemical shifts of −137 and −146 ppm, and relative intensities of 16% and 84%, respectively. These ^{19}F chemical shift values are consistent with Si–F bonding, as has been demonstrated in a number of crystalline and gas-phase compounds [15,16]. The structural assignment of the two resonances in Fig. 1(a) is not immediately obvious as these peaks have not been previously observed. However, an idea of the local symmetry of the fluorine environments can be gained by examining the line shape of the ^{19}F resonances in a static ^{19}F NMR spectrum. Such data for this glass are shown in Fig. 1(b) where the chemical shift anisotropy (CSA) of the line shape is characteristic of uniaxial symmetry around the Si–F bonds. This is consistent with the wideline ^{19}F NMR study of Duncan et al. [13] and indicates that most of the fluorine atoms participate in bonding as a single fluorine per silicon atom (i.e. symmetry precludes the presence of multiple fluorine atoms on any given silicon, as in $SiO_{2/2}F_2$). The disorder induced heterogeneous broadening of this line shape is indicative of the fact that there are multiple fluorine environments in the glass with a range of CSAs. Moreover, the broad static ^{19}F line shape of the glass makes it impossible to determine whether the CSA of the minor component in the ^{19}F MAS spectrum at −137 ppm is significantly different from that of the major component at −146 ppm. However, it is unlikely that there is a significant fraction of the total fluorine in the glass that are located at sites with non-uniaxial

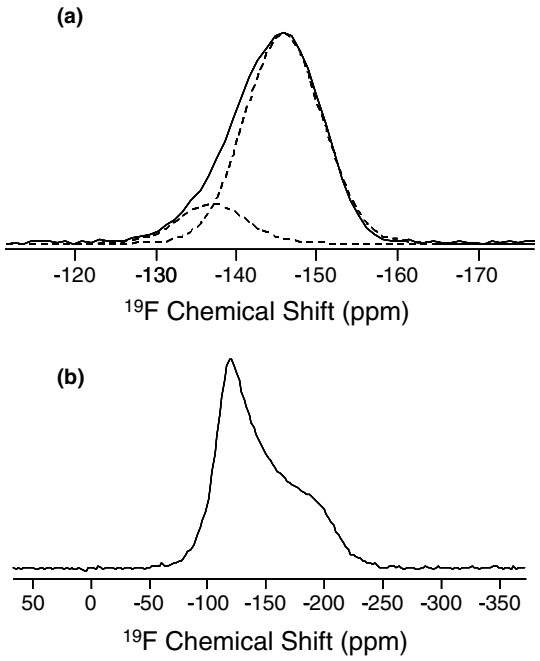

Fig. 1. ^{19}F NMR spectra of 3 wt% fluorine in a-SiO_2. (a) ^{19}F MAS NMR spectrum, in which dashed lines correspond to Gaussian fits to two fluorine resonances at −137 and −146 ppm. (b) Wideline ^{19}F NMR spectrum.

symmetry as we do not observe any distortion of the uniaxial line shape in Fig. 1(b).

Additional details of the Si–F bonding were obtained through $^{19}F \rightarrow {}^{29}Si$ CPMAS experiments, where the resulting ^{29}Si spectra contain resonances primarily from silicon atoms bonded directly to fluorine. The ^{29}Si CPMAS NMR spectra in Fig. 2 contain three distinct ^{29}Si resonances, the relative intensities of which change as a function of contact time in the CPMAS experiment. At short contact times, the enhanced signals are due to silicon atoms bonded directly to fluorine or those in very close proximity to fluorine. On the other hand, those resonances which grow in intensity with increasing contact time are due to silicon atoms at larger distances from the fluorine. The data in Fig. 2 demonstrate that two of the silicon environments, corresponding to the peaks at −103 and −125 ppm, are a result of Si–F bonding in the glass and the resonance at −112 ppm is the usual Q^4 group in a-SiO_2 [17], some of which are spatially close to the Si–F groups. The relative deshielding of the ^{29}Si NMR peak at −103 ppm with respect to the Q^4 peak at −112 ppm is consistent with the formation of a Q^3 species of the type $SiO_{3/2}F$. On the other hand the more shielded peak at −125 ppm most likely corresponds to silicon atoms with coordination numbers larger than four. The ^{29}Si chemical shift for silicon atoms fivefold coordinated to oxygen is known to be at around −150 ppm [18]. If one of these oxygen atoms is replaced by a terminal fluorine, as in some high silica zeolites, then the ^{29}Si chemical shift for the fivefold coordinated silicon is actually shifted downfield to a range of −115 to −150 ppm [19]. Therefore, the likely assignment of the ^{29}Si NMR peak at −125 ppm would be a fivefold coordinated silicon species of the type $SiO_{4/2}F$ where the central silicon is bonded to four bridging oxygens and one terminal fluorine. The relative intensities of these two silicon resonances, which are only quantitative in the MAS NMR data shown in Fig. 3 and not the CPMAS NMR data, are consistent with that of the two fluorine peaks in Fig. 1(a). This result thus indicates that the fluorine resonance at −146 ppm corresponds to the $SiO_{3/2}F$ group and the related silicon resonance is at −103 ppm. The second fluorine peak at −136 ppm corresponds to the −125 ppm silicon resonance, which is due to formation of penta-coordinated silicon with a single non-bridging fluorine atom added to the four bridging oxygen ligands. These measured ^{19}F chemical shift values are also in close agreement with the calculations of Liu and Nekvasil for a variety of Si–F bonding configurations including those with fivefold coordinated silicon [20].

We also observe these two structural species in the final glass structure obtained from the MD simulation of a 1.2 wt% fluorine-doped a-SiO_2. The picture in Fig. 4 shows a portion of the simulation cell, containing the fivefold coordinated silicon in $SiO_{4/2}F$ groups. The Si–F distance in this bonding scheme is quite long, on the order of 1.9–2.0 Å, which may also account for the relatively small shielding increase upon addition of an Si–F linkage to a Q^4 silicon. The $SiO_{3/2}F$ groups can be found in other parts of the simulation cell with typical Si–F distances of ~1.7 Å, consistent with the results obtained by Zirl and Garofalini in their simulations of fluorinated vitreous silica surfaces [14]. Due to the extremely fast quenching rates employed in MD simula-

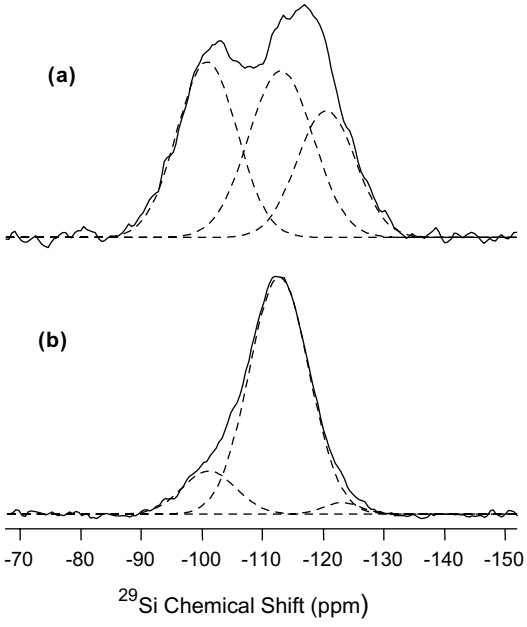

Fig. 2. $^{19}F \rightarrow {}^{29}Si$ CPMAS NMR spectra of 3 wt% fluorine in a-SiO_2 obtained using contact times of (a) 0.5 ms and (b) 10 ms. Dashed lines correspond to Gaussian fits with three ^{29}Si resonances at −103, −112 and −125 ppm.

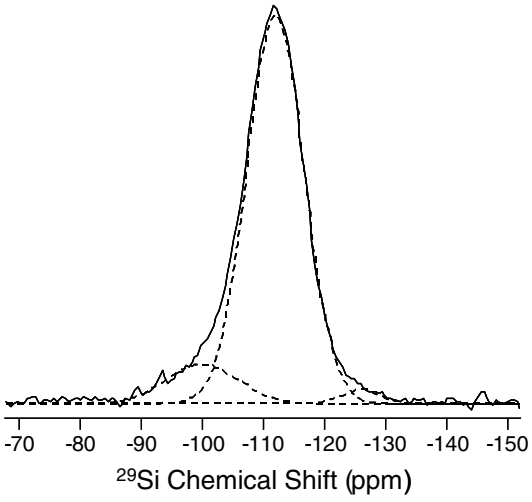

Fig. 3. ^{29}Si MAS NMR spectrum of 3 wt% fluorine in a-SiO_2. Dashed curves denote Gaussian fits to three distinct silicon peaks observed in the CPMAS NMR spectra in Fig. 2.

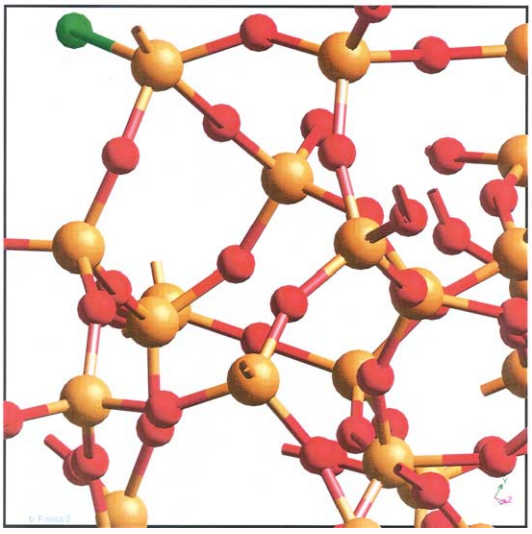

Fig. 4. Molecular dynamics simulation of F-doped a-SiO_2. A small portion of the simulation cell is pictured where in the upper left corner there is a view of the $SiO_{4/2}F$ penta-coordinated silicon structure. Silicon, oxygen and fluorine atoms are represented in yellow, red and green, respectively.

tions the final glass structures have the possibility to contain structural elements characteristic of high fictive temperatures. In the present case structures quenched from high simulation temperatures ($\geqslant 2500$ K) are found to contain an increasing fraction of free fluorine atoms in the simulation cell that are not bonded to the Si–O network. However, the effect of cooling rate or fictive temperature on the relative concentrations of the two types of Si–F species could not be evaluated in these simulations due to the time constraint involved in obtaining significantly slow cooling rates in computer simulations in general. It can be argued on the basis of bond valence calculations that another possible species that may form in F-doped a-SiO_2 is a fluorine atom in a bridging configuration, i.e. Si–F–Si linkages, although no evidence of the formation of such a species was observed in these simulations. The relative concentrations of $SiO_{3/2}F$ and $SiO_{4/2}F$ polyhedra (~6:1) as obtained from these MD simulations are found to be consistent with the relative peak intensities in Fig. 1(a) although such an agreement may be fortuitous especially if the relative concentrations of the two fluorine species is dependent on fictive temperature. Therefore, this combined NMR and MD simulation study of F-doped a-SiO_2 shows that the atomic structure of fluorine-doped a-SiO_2 consists mainly of a corner-shared continuous network of Q^4 tetrahedra, interrupted at places by replacement of a bridging oxygen with a non-bridging fluorine. In addition, there is a small fraction of fluorine atoms that are linked to the Q^4 tetrahedra without any rupture of the Si–O network, resulting in fivefold coordinated silicon.

These results have wide-ranging implications on our understanding of the structural and physico-chemical roles played by halogens in silicates and of the various technological applications of F-doped a-SiO_2. The main consequence of adding small quantities of fluorine is to depolymerize the silicate network through formation of non-bridging fluorine, consistent with formation of mostly $SiO_{3/2}F$ tetrahedra. This depolymerization accounts for substantial decreases in T_g and viscosity of F-doped a-SiO_2. Moreover, the formation of $SiO_{3/2}F$ units requires significant structural modification of the network and breaking of Si–O–Si linkages and, therefore, may play an important role in preferentially removing strained bonds from the network. It has been suggested in previous studies that removal of strained Si–O–Si linkages is responsible for increasing the transparency of silica in the ultraviolet on addition of fluorine [5]. The secondary structural role of fluorine involves the formation of fivefold coordinated silicon, which does not change the overall network connectivity, but nevertheless may play a significant role in controlling the viscous flow of these materials in the liquid state. For example, previous MD simulation studies have indicated that the mechanism of viscous flow in silicate liquids can be viewed as a co-operative bond breaking and reforming event where a likely transition state would involve silicon atoms in fivefold coordination [21]. It is tempting to speculate that in fluorinated silica the $SiO_{4/2}F$ unit may play a similar role in the melt, allowing for mass transport and viscous flow. The unusual bonding configuration of this $SiO_{4/2}F$ unit may also influence the optical properties of these materials. For example the susceptibility of these glasses towards formation of color centers on laser exposure is likely to increase with increasing concentration of this over-coordinated silicon species. This is because such species may act as high-energy precursors which would have a tendency to decay to the low-energy $SiO_{3/2}F$ configuration through laser assisted scission of a Si–O bond with the concomitant formation of a non-bridging oxygen hole center. An understanding of these structure–property relationships is crucial especially considering the current widespread use of F-doped silicas in long-haul telecommunications and next-generation photolithographic processes. We are currently expanding our studies to include a detailed examination of the effect of fluorine content and fictive temperature on the speciation of fluorine in F-doped a-SiO_2 [22].

4. Conclusion

In summary, these multi-nuclear high-resolution NMR studies have shown for the first time, the presence of multiple fluorine environments in fluorinated silica glass. The addition of fluorine tends to depolymerize the

silica network by replacing some of the bridging oxygen atoms with terminal Si–F groups, resulting in a drastic drop in viscosity and glass transition temperature. A small fraction of the fluorine is bonded to silicon atoms containing four bridging oxygen atoms, resulting in fivefold coordinated silicon of the type $SiO_{4/2}F$. This type of structure may play a key role as a transition state in controlling the atomistic mechanism of viscous flow of fluorine-containing silicate melts. These two types of fluorine species are also likely to be closely linked to the performance of F-doped a-SiO_2 in terms of its optical transparency and its susceptibility to laser damage.

References

[1] J.W. Fleming, D.L. Wood, Appl. Opt. 22 (1983) 3102.
[2] M. Ogai, A. Iino, K. Matsubara, J. Tamura, M. Koguchi, S. Nakamura, E. Kinoshita, J. Lightwave Technol. 6 (1988) 1455.
[3] M.J. Shapiro, S.V. Nguyen, T. Matsuda, D. Dobuzinsky, Thin Solid Films 270 (1995) 503.
[4] J.A. McClay, A.S.L. McIntyre, Solid State Technol. 42 (1999) 57.
[5] H. Hosono, M. Mizuguchi, L. Skuja, Opt. Lett. 24 (1999) 1549.
[6] T. Katsuo, Y. Satohito, T. Kimio, Bull. Jpn. Pet. Inst. 12 (1970) 136.
[7] D.B. Dingwell, C.M. Scarfe, D.J. Cronin, Am. Mineral. 70 (1985) 80.
[8] D.B. Dingwell, Am. Mineral. 74 (1989) 333.
[9] J.C. Bailey, Chem. Geol. 19 (1977) 1.
[10] K. Aoki, K. Ishiwaka, S. Kanisawa, Contrib. Mineral. Petrol. 76 (1998) 53.
[11] P. Dumas, J. Corset, W. Carvalho, Y. Levy, Y. Neuman, J. Non-Cryst. Solids 47 (1982) 239.
[12] C.A.M. Mulder, R.K. Janssen, P. Bachmann, D. Leers, J. Non-Cryst. Solids 72 (1985) 243.
[13] T.M. Duncan, D.C. Douglass, R. Csencsits, K.L. Walker, J. Appl. Phys. 60 (1986) 130.
[14] D.M. Zirl, S.H. Garofalini, J. Non-Cryst. Solids 122 (1990) 111; B.P. Feuston, S.H. Garofalini, J. Chem. Phys. 91 (1989) 564; B.P. Feuston, S.H. Garofalini, J. Chem. Phys. 89 (1988) 5818.
[15] T.J. Kiczenski, J.F. Stebbins, J. Non-Cryst. Solids 306 (2002) 160.
[16] R.B. Johannesen, T.C. Farrar, F.E. Brinckman, T.D. Coyle, J. Chem. Phys. 44 (1966) 962.
[17] L.F. Gladden, T.A. Carpenter, S.R. Elliott, Philos. Mag. B 53 (1986) L81.
[18] J.F. Stebbins, Nature 351 (1991) 638.
[19] H. Koller, A. Wölker, L.A. Villaescusa, M.J. Díaz-Cabañas, S. Valencia, M.A. Camblor, J. Am. Chem. Soc. 121 (1999) 3368.
[20] Y. Liu, H. Nekvasil, Am. Mineral. 87 (2002) 339.
[21] S. Brawer, Relaxation in Viscous Liquids and Glasses, American Ceramic Society, Columbus, OH, 1985.
[22] R.E. Youngman, S. Sen, J. Non-Cryst. Solids (submitted for publication).